

Dyadic Cantor set and its kinetic and stochastic counterpart

M. K. Hassan¹, N. I. Pavel¹, R. K. Pandit¹ and J. Kurths²

¹ *University of Dhaka, Department of Physics, Theoretical Physics Group, Dhaka 1000, Bangladesh*

² *Potsdam Institute for Climate Impact Research, Telegrafenberg A31, 14473 Potsdam, Germany*

(Dated: January 3, 2014)

Firstly, we propose and investigate a dyadic Cantor set (DCS) and its kinetic counterpart where a generator divides an interval into two equal parts and removes one with probability $(1 - p)$. The generator is then applied at each step to all the existing intervals in the case of DCS and to only one interval, picked with probability according to interval size, in the case of kinetic DCS. Secondly, we propose a stochastic DCS in which, unlike the kinetic DCS, the generator divides an interval randomly instead of equally into two parts. Finally, the models are solved analytically; an exact expression for fractal dimension in each case is presented and the relationship between fractal dimension and the corresponding conserved quantity is pointed out. Besides, we show that the interval size distribution function in both variants of DCS exhibits dynamic scaling and we verify it numerically using the idea of data-collapse.

PACS numbers: 61.43.Hv, 64.60.Ht, 68.03.Fg, 82.70.Dd

I. INTRODUCTION

The world we live in is not restricted to Euclidean geometry like lines, squares, rectangles, circles, semi-circles, spheres, etc only. Instead, there are curves twisted so wildly that they occupy plane not a line, there are surfaces folded so badly that they occupy space not a plane, there are objects so stringy or ramified that their constituents are distributed scarcely not uniformly. Indeed, most of the natural objects we see around us are so complex in shape and structure that Euclidean geometry is not sufficient to describe them. Many of these objects used to be described as geometrically chaotic, since they are not just merely complex but often contain different degrees of complexity. In 1975 Mandelbrot introduced the idea of fractal to describe these geometrically chaotic objects and it has revolutionized the notion of geometry forever. It helps us appreciate the fact that there exists some kind of order even in seemingly disordered and apparently bewildering objects [1, 2]. Prior to the inception of the idea of fractal, geometry remained one of the main branches of mathematics. However, soon after its inception, it has attracted mathematicians, physicists, and engineers all alike and hence generated a widespread interest in subjects like physics, chemistry, biology, earth science, economics, etc [3–5]. The exact definition of fractal remains elusive even after more than thirty five years. This is partly because Mandelbrot himself was somewhat reluctant to confine it within the boundaries of a mere definition. He nevertheless proposed that fractal is a geometric object with irregular shape made of parts similar to the whole, in some sense.

The idea of the Hausdorff-Besicovitch dimension, however, plays a pivotal role in defining fractal. Consider that the measure H_d describes the size of the set of points that constitute an Euclidean object. We can quantify the size of the measure H_d by using a d -dimensional hypercube of linear size δ as an yardstick. We can write the measure H_d in terms of the number $N(\delta)$ needed to cover

the object as

$$H_d = \sum \delta^d = N(\delta)\delta^d, \quad (1)$$

where δ^d is the test function [6]. It can be easily shown that $N(\delta)$ for Euclidean objects always satisfies

$$N(\delta/n) = n^{d_E} N(\delta) \quad \text{with} \quad d_E = 1, 2, 3, \quad (2)$$

and hence $N(\delta)$ is a homogeneous function. One can explicitly prove that only a power-law solution for $N(\delta)$ can satisfy Eq. (2) [7]. Indeed, it is easy to check that

$$N(\delta) \sim \delta^{-d_E}, \quad (3)$$

is a solution of Eq. (2). It implies the dimension d_E of an object can be defined as the slope of the plot of $N(\delta)$ vs δ in the log – log scale. Obviously, the slope d_E of such a plot for Euclidean objects will always be an integer quantity. However, there exists another class of natural or man-made objects for which the slope of the same plot may assume a non-integer value which we typically denote by d_f . We can therefore generalize the solution for $N(\delta)$ upon replacing d_E by an unconstrained exponent D . Using it in Eq. (1) we find that there exists a critical dimension $d = D$, known as the Hausdorff-Besicovitch (H-B) dimension, for which the measure M_d neither vanishes nor diverges as $\delta \rightarrow 0$ [6]. Thus, an object is fractal if the H-B dimension $D = d_f$ assumes a non-integer value and at the same time it is less than the dimension of the space where the object is being embedded.

One of the best known text-book example of fractal is the triadic Cantor set. It starts with an initiator, typically an interval of unit size, and a generator that divides it into three equal parts and remove the middle third. The generator is then applied at each successive step to all the available smaller intervals over and over again. The resulting set has a non-integer H-B dimension $d_f = \ln 2 / \ln 3$ with numerical value less than that of the space $d = 1$ where the set is embedded [6]. Besides its

pedagogical importance, the Cantor set problem has also been of theoretical and practical interest [8–11]. However, as far as natural fractals are concerned, the Cantor set lacks at least in two ways. Firstly, it does not appear through evolution in time, although fractals in nature do so. Secondly, it is not governed by any sort of randomness throughout its construction process, while natural fractals always occur through some kind of evolution accompanied by some randomness. Note that nature likes freedom not determinism. Indeed, it is well understood that in our world almost nothing is stationary or strictly deterministic. Most natural objects we see around us are seemingly complex in character albeit they are governed by simple rules. Note that it is the simple rules when repeated over and over again that make the resulting system look mighty complex in the end.

Motivated by the importance and impact of the Cantor set, we investigate here a couple of its interesting variants in which probability, time and randomness are incorporated in a logical progression. To this end, we first propose dyadic Cantor set (DCS) which is simpler than the much known triadic Cantor set (TCS) since dividing into two is undeniably simpler than dividing into three in any sense. We then introduce the kinetic counterpart of the DCS by applying the generator to only one interval at each step by picking it preferentially with respect to interval size. The sequential application of the generator immediately introduces time as one parameter in the problem and hence it helps us to understand its impact on the resulting fractal and various other observable quantities. Finally, we introduce spatial randomness by modifying the generator such that it divides an interval randomly into two parts instead of dividing into two equal parts and apply it sequentially like kinetic DCS. Consequently, it now incorporates both time and spatial randomness in the system making it a stochastic counterpart of the DCS. Each variants of the DCS are solved analytically to obtain the fractal dimension and to show self-similarity. Analytic results, especially the self-similar properties, are verified numerically by invoking the idea of data collapse.

The remainder of this article is organized as follows. In section II, we propose the dyadic Cantor set and discuss various properties. In section III, we propose the kinetic counterpart of the dyadic Cantor set and solve it exactly to obtain the fractal dimension and various other properties. In section IV, we investigate the stochastic counterpart of the dyadic Cantor set and solve it analytically. We also propose its exact algorithm to solve it by numerical simulation to verify our analytical results. We then revisit the kinetic DCS problem in section V with an aim to check whether it also exhibits dynamic scaling or not. Finally, in section VI, we give a general discussion and summary of the work.

II. DYADIC CANTOR SET (DCS)

In this section, we first define the dyadic Cantor set (DCS) and then investigate its various aspects. It starts with an initiator which is typically an interval of unit length $[0, 1]$. The generator then divides the initiator into two equal parts and deletes one, say the right half, with probability $(1 - p)$. After step one, the system on average will have $(1 + p)$ number of sub-intervals of size $1/2$, since the right half interval remains there in step one with probability p . In the next step, the generator is applied to each of the $(1 + p)$ available sub-intervals to divide them into two equal parts and remove the right half from each of the $1 + p$ intervals with probability $(1 - p)$. The system will then have on average $(1 + p)^2$ number of intervals of size $1/4$ as $(1 - p)(1 + p)$ number of intervals of size $1/4$ are removed on average. The process is then continued over and over again by applying the generator on all the available intervals at each successive step recursively.

Finding the fractal dimension of the DCS problem is as simple as its definition. According to the construction of the DCS process, there are $N = (1 + p)^n$ intervals in the n th generation and they are of size $\delta = 2^{-n}$. The most convenient yard-stick to measure the size of the set in the n th step is the mean interval size $\delta = 2^{-n}$. Expressing N in favour of δ by using $\delta = 2^{-n}$, we find

$$N(\delta) \sim \delta^{-d_f}, \quad (4)$$

where $d_f = \frac{\ln(1+p)}{\ln 2}$. Note that the exponent d_f is non-integer for all $0 < p < 1$ and at the same time it is less than the dimension of the space $d = 1$, where the set is embedded. It is therefore the fractal dimension of the resulting DCS which does not fill up the unit interval continuously to constitute a line. Unlike the triadic Cantor set where the Cantor dusts are distributed in a strictly self-similar fashion, the Cantor dusts in the dyadic Cantor set are distributed in a random fashion, yet it is self-similar in the statistical sense only.

One of the most interesting aspects of the triadic Cantor set is worth mentioning here. The intervals which are removed from the triadic Cantor set are of size $1/3, 2/9, 4/27, \dots$ etc and if we add them up we get

$$\frac{1}{3} \sum_{n=0}^{\infty} \left(\frac{2}{3}\right)^n = 1. \quad (5)$$

This is the size of the initiator and hence it means that there is nothing left in the triadic Cantor set, since the sum of the sizes that are removed equals the size of the initiator. Interestingly, we find that a similar argument holds for dyadic Cantor set too. For instance, on the average in step one the amount of size removed is $\frac{1-p}{2}$, in step two the total amount of size removed is $\frac{(1-p)(1+p)}{4}$, in step three it is $\frac{(1-p)(1+p)^2}{8}$, in step four it is $\frac{(1-p)(1+p)^3}{16}$

and so on. If we add these intervals we have

$$\frac{(1-p)}{2} \sum_{n=0}^{\infty} \left(\frac{1+p}{2}\right)^n = 1 \quad (6)$$

which is again the size of the initiator. It means, like in the triadic Cantor set, there is hardly anything left in the DCS. However, we will show later that there are still tons of members in the set.

III. KINETIC DYADIC CANTOR SET

We now ask: What happens if the generator of the DCS is applied to only one interval at each step instead of applying it to all the available intervals in each successive step? Clearly, the spatial distribution of the remaining intervals will be very different from the one created by the DCS problem. Yet the question is: Will the number N needed to cover the set by a yardstick, say the mean interval size δ , still exhibit a power-law against δ ? If yes, will the exponent *vis-a-vis* the fractal dimension be the same as that of the DCS? To find a definite answer to these questions, it is important to appreciate the fact that after step one and beyond the system will have intervals of different sizes and hence it raises a further question: How do we choose one interval when the system has intervals of different sizes? To this end, we choose the most generic case whereby an interval is picked preferentially with respect to their sizes.

The algorithm of the kinetic DCS problem can be defined as follows. Like DCS it also starts with an initiator of a unit interval $[0, 1]$. In the first step the generator divides the initiator into two sub-intervals of equal size and removes one of the part, say the right half, with probability $(1-p)$. There are now $(1+p)$ intervals each of size $1/2$. In the next step we generate a random number R from the open interval $(0, 1)$ and find which of the $(1+p)$ sub-intervals contains this number R in order to ensure that the interval is picked preferentially according to their sizes. If R is found within the interval $[0, \frac{1}{2}]$ then we pick it; else we pick the right interval if it has not already been removed. Say, the left interval contains R and hence we pick that and the generator is then applied onto it only. In any case, time is increased by one unit even if R is found within the interval that has been removed in which case the generator is not applied at all.

In order to study the kinetic DCS problem analytically, we use the binary fragmentation equation [12, 13]

$$\begin{aligned} \frac{\partial c(x, t)}{\partial t} = & -c(x, t) \int_0^x dy F(y, x-y) \\ & + 2 \int_x^\infty dy F(x, y-x) c(y, t), \end{aligned} \quad (7)$$

where $c(x, t)dx$ is the number of intervals within the size range x and $x+dx$ at time t and $F(x, y)$ is the fragmentation kernel that specifies the rate and the rules of the

fragmentation process. The first term on the right hand side of the above equation describes the loss of interval of size x due to its breakup into two smaller intervals, while the second term describes the gain of interval of size x due to breakup of an interval of size $y > x$ into two smaller pieces ensuring that one of the two smaller intervals is of size x . The factor 2 in the gain term implies that at each time step two intervals are produced out of one interval. However, in the context of the present model we need to replace the factor 2 of Eq. (7) by $(1+p)$ to ensure that on the average at each breaking event $(1+p)$ number of new intervals are produced. Next, we need to choose the following kernel

$$F(x, y) = (x+y)\delta(x-y), \quad (8)$$

to ensure that at each breaking event an interval is picked preferentially with respect to interval size and divide it into two equal pieces. Using the two facts in Eq. (7) we obtain

$$\frac{\partial c(x, t)}{\partial t} = -\frac{x}{2}c(x, t) + 2x(1+p)c(2x, t), \quad (9)$$

which is the required fitting equation that describes the kinetic DCS problem.

We now find it convenient to incorporate the definition of the moment

$$M_n(t) = \int_0^\infty x^n c(x, t) dx, \quad (10)$$

in Eq. (9) which gives the rate equation for $M_n(t)$ that reads as

$$\frac{dM_n(t)}{dt} = -\left[\frac{1}{2} - \frac{(1+p)}{2^{(n+1)}}\right] M_{n+1}(t). \quad (11)$$

This equation reveals that there exists a value of $n = n^*$ for which the moment M_{n^*} is a conserved quantity. The value of n^* can be found simply by finding the root of the following equation

$$\frac{1}{2} - \frac{(1+p)}{2^{(n^*+1)}} = 0. \quad (12)$$

Solving it we obtain $n^* = \frac{\ln(1+p)}{\ln 2}$ implying that the moment $M_{\frac{\ln(1+p)}{\ln 2}}(t)$ is a conserved quantity. To verify it numerically we denote the sizes of all the surviving intervals at the j th step as $x_1, x_2, x_3, \dots, x_{N_j}$ starting from the left most till the right most within $[0, 1]$ in order to avoid the use of $c(x, t)$ in the definition of the moment. The n^* th moment then is

$$M_{n^*} = \sum_{i=1}^{N_j} x_i^{n^*}, \quad (13)$$

which is indeed a conserved quantity according to Fig. (1). However, it is worth mentioning that the numerical value of the conserved quantity $M_{\frac{\ln(1+p)}{\ln 2}}(t)$ is not the

same at every independent realization. The question remains: Why the index of the moment $n^* = \frac{\ln(1+p)}{\ln 2}$ is so special? To find an answer to this question we invoke the idea of fractal analysis below.

It is expected that the kinetic DCS problem too, like the simple DCS, will generate fractal in the long time limit and hence it must possess self-similarity as it is an essential property of fractal. That is, the various moments of $c(x, t)$, which correspond to observable quantities, should exhibit a power-law relation with time, since dimensional functions are always power-law monomial in character. We therefore can write a tentative solution for the n th moment as

$$M_n(t) \sim A(n)t^{\alpha(n)}. \quad (14)$$

If we insist that it must obey the conservation law, $M_{\frac{\ln(1+p)}{\ln 2}} = \text{const.}$ then the exponent $\alpha(n)$ must satisfy $\alpha(n^*) = 0$. Substituting Eq. (14) in Eq. (11) yield the following recursion relation

$$\alpha(n+1) = \alpha(n) - 1. \quad (15)$$

Iterating it subject to the condition that $\alpha(n^*) = 0$ gives

$$\alpha(n) = -\left(n - \frac{\ln(1+p)}{\ln 2}\right). \quad (16)$$

We therefore now have an explicit asymptotic solution for the n th moment

$$M_n(t) \sim t^{-\left(n - \frac{\ln(1+p)}{\ln 2}\right)}. \quad (17)$$

It means that the number of intervals $N(t) = M_0(t)$ grows with time as

$$N(t) \sim t^{\frac{\ln(1+p)}{\ln 2}}, \quad (18)$$

revealing that there exists a non-trivial relation between the number of intervals N and the time t . On the other hand we find that the mean interval size $\delta = M_1(t)/M_0(t)$ decreases with time as

$$\delta(t) \sim t^{-\gamma}, \quad (19)$$

where the exponent $\gamma = 1$.

To verify Eq. (18) numerically we plot $\ln N$ vs $\ln t$ in Fig (2) and find a straight line with slope exactly equal to $\ln(1+p)/\ln 2$ as expected according to Eq. (18). In fractal analysis, one usually seeks for a power-law relation between the number $N(\delta)$ and a suitable yard-stick size δ . The mean interval size δ is definitely the best choice for the yard-stick. To find the required relation we therefore eliminate t from Eq. (18) in favour of δ given by Eq. (19) and we immediately find that N exhibits the same power-law $N \sim \delta^{-d_f}$ as we found in the case of DCS including the exponent $d_f = \frac{\ln(1+p)}{\ln 2}$. It implies that the value of the index n^* of the conserved quantity is actually the fractal dimension. One could not help but check about

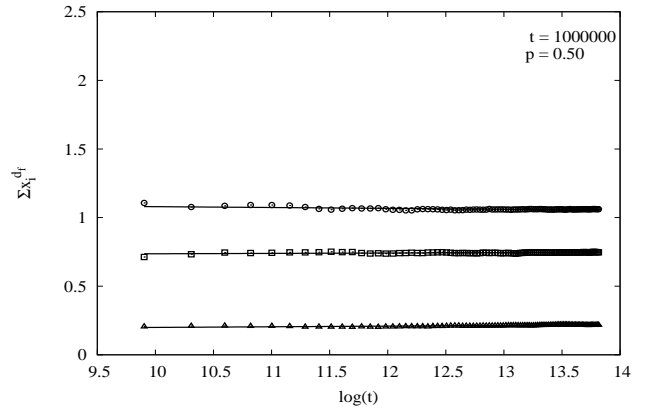


FIG. 1: The three horizontal lines for three independent realizations for the same p value show that the d_f th moment M_{d_f} of the remaining intervals, where $d_f = \ln(1+p)/\ln 2$, is a conserved quantity as suggested by Eq. (17). However, note that the numerical value of M_{d_f} assumes different numerical value at each independent realization.

the d_f th moment in the DCS case too. In this case the d_f th moment in the n th step is

$$M_{d_f} = \sum_{n=1}^{(1+p)^n} x_i^{d_f} = 1, \quad (20)$$

and hence it is indeed a conserved quantity since all the intervals are of same size regardless of the n value. The same is also true for the triadic Cantor set and one can easily verify it by setting $x_i = 3^{-n}$, $N = 2^n$ and $d_f = \ln 2/\ln 3$. This is surprising in the sense that on one hand the sum of all the intervals which are removed is equal to the size of the initiator revealing there is nothing left in the set. On the other hand, the d_f th moment M_{d_f} in all cases is a conserved quantity revealing that the system still has tons of intervals. The connections between the fractal dimension and the conserved quantity was first reported by Ben-Naim and Krapivsky in the context of the stochastic Cantor set [14]. Later, we found such connections to be true in many different variants of fragmentation and aggregation processes [15–20].

IV. STOCHASTIC DYADIC CANTOR SET

It is true that fractal in the DCS has some form of spatial randomness albeit the intervals at any stage of the construction process are of equal size. In contrast, intervals in the kinetic DCS are distributed not only randomly but they are also of different size at any given stage. Yet, we find that they share the same fractal dimension owing to the same deterministic rule in the definition of the generator. Nature do not like determinism rather it likes to enjoy some form of freedom in the selection process. Freedom in the present context means the liberty to divide an interval randomly. We therefore ask: What if we

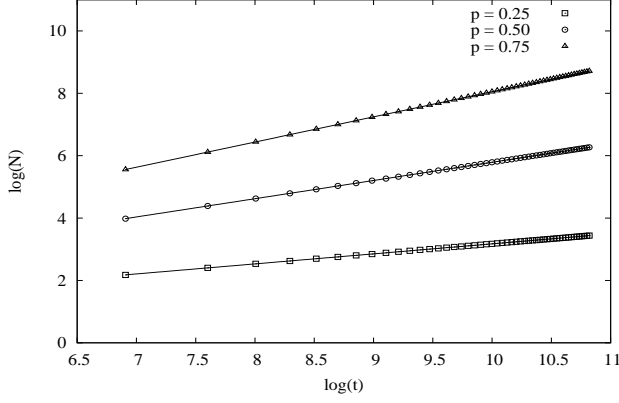


FIG. 2: Log-log plot of the interval number N vs time t are drawn for the kinetic DCS using three different p values. The lines have slope equal to fractal dimension $d_f = \ln(1+p)/\ln 2$, revealing that $N(t) \sim t^{d_f}$ as predicted by Eq. (18).

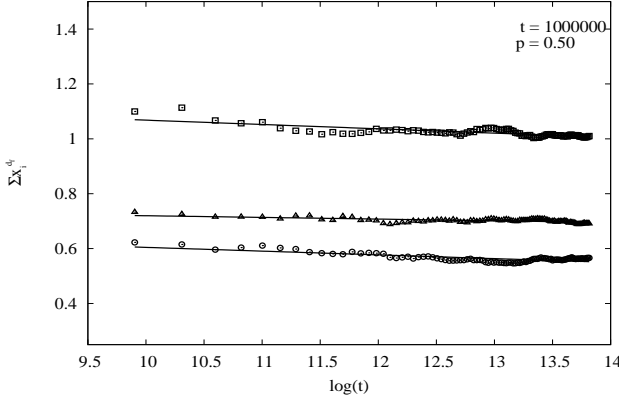


FIG. 3: Plot of the p th moment $M_p(t)$ of the remaining intervals as a function of time, where p is the fractal dimension of the stochastic DCS, showing that $M_p(t)$ is a conserved quantity in the long-time limit. The three distinct parallel lines for the same probability p reveal that the numerical value of the conserved quantity $M_p(t)$, like kinetic DCS, is different in each independent realization.

use a generator that divides an interval randomly into two smaller intervals instead of dividing it into two equal intervals? To this end we propose the following stochastic dyadic Cantor. We start the process with an initiator of unit interval $[0, 1]$ as before but unlike the previous cases the generator here divides an interval randomly into two pieces and removes one with probability $(1 - p)$. The algorithm of this model is exactly the same as the one for kinetic DCS except the fact that the generator always divides an interval randomly into two parts instead of dividing into two equal parts.

We can make Eq. (7) describing the rules of the stochastic DCS problem if we only choose

$$F(x, y) = 1, \quad (21)$$

and at the same time replace the factor 2 of the gain term

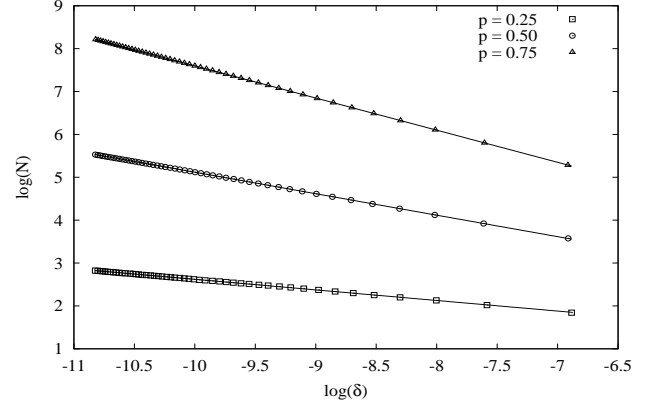


FIG. 4: Log-log plot of the interval number N vs yard-stick size δ using simulation data for three different p values and the same initial condition. The lines have slopes $d_f = p$ depicting that $N(\delta) \sim \delta^{-d_f}$ and hence this is in perfect agreement with our analytical result given by Eq. (25).

again by $(1 + p)$. The master equation for the stochastic DCS then is

$$\frac{\partial c(x, t)}{\partial t} = -xc(x, t) + (1 + p) \int_x^\infty c(y, t) dy. \quad (22)$$

The stochastic counterpart of the dyadic Cantor set is much simpler to solve analytically than the stochastic counterpart of the triadic Cantor set which was first proposed and solved analytically by Ben-Naim and Krapivsky [20, 21]. However, we for the first time give an exact algorithm of the model and focus primarily on verifying the various analytical results by extensive numerical simulation. Like before we once again incorporate the definition of the n th moment in the rate equation to obtain

$$\frac{dM_n(t)}{dt} = -\left[1 - \frac{(1 + p)}{(n + 1)}\right] M_{n+1}(t). \quad (23)$$

Following the same procedure as for the kinetic DCS problem, we obtain the asymptotic solution for the n th moment

$$M_n(t) \sim t^{(n-p)z} \quad \text{with} \quad z = -1, \quad (24)$$

which implies that p is the special value of n for which $M_p(t)$ is a conserved quantity (see Fig (3)).

Note that the solution for $M_n(t)$ given by Eq. (24) clearly suggests that the dynamics of the stochastic DCS too governed by a conservation law namely the moment of order $n = p$ is a conserved quantity. The solution for $M_n(t)$ also suggests that the mean interval size $\delta(t)$ decays following the same power-law and the same exponent as in Eq. (19). Using it as the yard-stick we find that the number $N(\delta)$ needed to cover the resulting set scales as

$$N(\delta) \sim \delta^{-d_f}, \quad (25)$$

with $d_f = p$ revealing that the index of the conserved quantity is again equal to the fractal dimension (see Fig. (4)). Note that the fractal dimension $d_f = p$ is always less than $\frac{\ln(1+p)}{\ln 2}$ regardless of the value of p . Hence we can conclude that the fractal dimension of the stochastic fractal is always less than that of its recursive or kinetic counterpart. Once again we find that the moment of order equal to fractal dimension M_{d_f} is a conserved quantity. It seems quite like a rule than otherwise as we have found it to true also in the case of its opposition phenomena namely in aggregation [15–20].

We shall now apply the Buckingham π -theorem to obtain a scaling solution for $c(x, t)$ as it provides a deeper insight into the problem [22]. Note that according to Eq. (22) the governed parameter c depends on three parameters x , t and p of which only the former two are dimensional. However, the knowledge about the decay law for the mean interval size implies that one of the parameter, say x , can be expressed in terms of t since we find $\delta = t^{-1}$ must bear the dimension of the interval size x . We therefore can define a dimensionless governing parameter

$$\xi = \frac{x}{t^{-1}}, \quad (26)$$

and a dimensionless governed parameter

$$\Pi = \frac{c(x, t)}{t^\theta}. \quad (27)$$

The numerical value of the right side of the above equation remains the same even if the unit time t is changed by some factor, say μ for example, since the left hand side is a dimensionless quantity. It means that the two parameters x and t must combine to form a dimensionless quantity $\xi = x/t^{-1}$ and the dimensionless parameter Π only depends on ξ . In other words we can write

$$\frac{c(x, t)}{t^\theta} = \phi(x/t^{-1}), \quad (28)$$

which leads to the following dynamic scaling form

$$c(x, t) \sim t^\theta \phi(x/t^{-1}), \quad (29)$$

where the exponent θ is fixed by some conservation law and $\phi(\xi)$ is known as the scaling function. Indeed, substituting Eq. (29) in the conservation law

$$\int_0^\infty x^p c(x, t) dx = \text{const.}, \quad (30)$$

we immediately obtain that $\theta = 1 + p$.

We now substitute Eq. (29) in Eq. (22) and find that it reduces the partial integro-differential equation into an ordinary integro-differential equation for the scaling function $\phi(\xi)$ given by

$$\xi \frac{d\phi(\xi)}{d\xi} + (\xi + (1 + p))\phi(\xi) = (1 + p) \int_\xi^\infty \phi(\eta) d\eta. \quad (31)$$

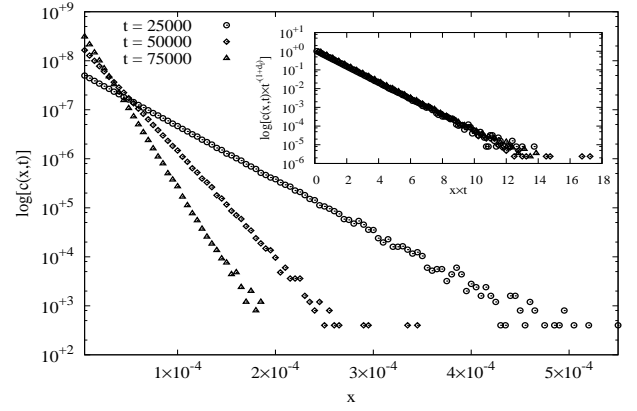


FIG. 5: Log-linear plot of the interval size distribution function $c(x, t)$ vs x for the stochastic DCS using data at three different times. Inset shows the collapse of the same data when we plot $t^{-(1+p)}c(x, t)$ vs xt in the Log – linear scale which clearly verifies that the solution for $c(x, t)$ given by Eq. (35).

This is much simpler to solve than solving Eq. (22). To simplify it even further, we differentiate Eq. (31) with respect to ξ getting

$$(-\xi) \frac{d^2\phi(\xi)}{d(-\xi)^2} + ((2 + p) - (-\xi)) \frac{d\phi(\xi)}{d(-\xi)} - (2 + p)\phi(\xi) = 0, \quad (32)$$

This is exactly Kummer's confluent differential equation whose solution is given by

$$\phi(\xi) = {}_1F_1(2 + p; 2 + p; -\xi), \quad (33)$$

where ${}_1F_1(a; c; z)$ is called the Kummer's confluent hypergeometric function [23]. We find that in the limit $\xi \rightarrow \infty$ the solution for the function $\phi(\xi)$ assumes a simple form

$$\phi(\xi) = e^{-\xi}. \quad (34)$$

Using it in Eq. (29) we find

$$c(x, t) \sim t^{1+p} e^{-xt}, \quad (35)$$

which essentially implies that it exhibits dynamic scaling in the limit $t \rightarrow \infty$ [24]. To verify it we have drawn a histogram of the distribution function $c(x, t)$ collecting data for fixed a time in the log-linear scale and found a set of straight line since for a fixed time the interval size distribution function $c(x, t)$ should decay exponentially (see Fig. (5)).

One of the key features of fractal is that it must be self-similar. In general, by self-similarity we mean that a suitably chosen part of an object represents the whole. The question is: What do we mean by self-similarity in stochastic fractal? Note that stochastic fractal such as stochastic DCS is not static rather it evolves with time. By self-similarity in such a case, we mean that it is similar with itself at different times. Note that the same system at different times are similar if the numerical values

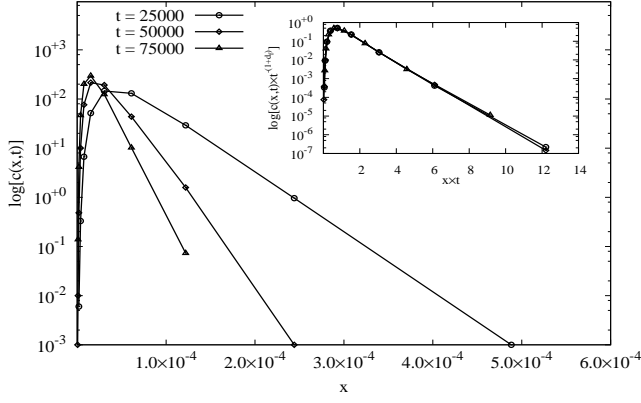


FIG. 6: Log – linear plots of the interval size distribution function $c(x, t)$ of the kinetic DCS is drawn as a function of x for three different times. In inset we show that the three distinct curves for three different system sizes collapsed onto a single universal curve if we plot $t^{-(1+d_f)}c(x, t)$ vs xt . It implies that the system exhibits self-similarity with respect to time.

of various dimensional governing parameters are different, however, the numerical values of the corresponding dimensionless quantities must coincide. Indeed, in the case of stochastic DCS the numerical value of the governed parameter $c(x, t)$ for a given value of the governing parameter x is different at different time which can easily be seen in Fig (5). However, the numerical value of the corresponding dimensionless governed parameter $c(x, t)/t^{1+p}$ and the dimensionless governing parameter xt should coincide. That is, all the distinct sets of curve of $c(x, t)$ as a function of x at different times should collapse onto one single curve if we plot $c(x, t)/t^{1+p}$ as a function of xt . This is exactly what we have shown in the inset of Fig. (5) and found that the data points of all the three distinct curves of Fig (5) merge superbly onto a single universal curve which is essentially the scaling function $\phi(x)$.

V. SELF-SIMILARITY IN KINETIC DCS

What about self-similarity in the kinetic dyadic Cantor set? Does it also exhibit dynamic scaling? A closer look at the solution $c(x, t) \sim t^{1+p}e^{-xt}$ for the stochastic DCS perhaps can guide us to write the solution of $c(x, t)$ for the kinetic DCS. To this end, we find it instructive to express $c(x, t)$ of stochastic DCS in terms of the mean interval size $\delta(t)$ and the fractal dimension d_f

$$c(x, t) \sim \delta^{-(1+d_f)} \phi(x/\delta(t)), \quad (36)$$

as we know $\delta \sim t^{-1}$ and $d_f = p$ for stochastic DCS. That is, substituting $d_f = \ln(1+p)/\ln 2$ and $\delta \sim t^{-1}$ for kinetic DCS we can immediately write the expected solution for it as

$$c(x, t) \sim t^{1+\frac{\ln(1+p)}{\ln 2}} \phi(xt). \quad (37)$$

To verify it, we plot first $c(x, t)$ vs x for three different times (see Fig. (6)) and then plot the corresponding dimensionless quantities $c(x, t)/t^{1+\frac{\ln(1+p)}{\ln 2}}$ vs xt . We once again find a superb data-collapse which is shown in the inset of the Fig (6) revealing that the fractal generated by kinetic DCS too exhibits a dynamic scaling *vis-a-vis* self-similarity.

VI. DISCUSSION AND SUMMARY

In this section we attempt to summarize and put all our findings into perspective. In this article we proposed a dyadic Cantor set and then its kinetic and stochastic counterpart. In these models we incorporated probability, time and randomness in such a way that a logical flow can easily be appreciated. Firstly, We solved the DCS problem by using probabilistic argument and found that it emerges as a fractal of dimension $d_f = \ln(1+p)/\ln 2$. Then we solved the kinetic and stochastic DCS using the rate equation approach and found that the resulting systems emerge as fractal of dimensions $d_f = \ln(1+p)/\ln 2$ and $d_f = p$ respectively. Our studies reveal that the inclusion of kinetics alone does not alter the value of the fractal dimension. However, inclusion of randomness in the generator of the stochastic DCS does change the value of the fractal dimension and found that it is always smaller than that of the DCS or the kinetic DCS.

Besides giving exact analytical expressions for fractal dimensions we have also given solutions for the interval size distribution function $c(x, t)$ for both kinetic and stochastic DCS problem alongside numerical simulations which fully support our solutions. In particular, we have shown that the distribution function $c(x, t)$ evolves to a state where it exhibits dynamic scaling $c(x, t) \sim t^{1+p}e^{-xt}$. We used the idea of data-collapse to verify it numerically. For instance, we have drawn $c(x, t)$ vs x using data for a fixed time and found a distinct set of curves for every different time of the process. However, these distinct curves collapsed onto a single universal curve when we expressed $c(x, t)$ in unit of t^{1+p} and x in unit of t^{-1} . It implies that the system is similar to itself at different time and hence we say that such systems exhibit self-similarity. It readily implies that the solution is independent of initial condition. We have shown that the self-similar properties in all three cases are accompanied by conservation laws and interestingly the value of the fractal dimension d_f coincide with the index of the conserved quantity M_{d_f} . The numerical value of the conserved quantity M_{d_f} , however, is found different at each realization. We have then checked if the d_f th moment is also a conserved in the dyadic and traditional triadic Cantor set and found that it is obeyed in both the cases as well. We think it is quite safe to argue that when systems evolve and yet preserve self-similarity then the dynamics of the system must be governed by conservation law.

To explain why the quantity M_{d_f} always remains constant we find it useful to consider a simple dimensional

analysis. According to Eq. (35) the physical dimension of $c(x, t)$ is $[c] = L^{-(1+d_f)}$ since $[s(t)] = L$. To know why the quantity $M_{d_f} = \int_0^\infty x^{d_f} c(x, t) dx$ is a conserved quantity we find it convenient to look into the physical dimension of its differential quantity $dM_{d_f} = x^{d_f} c(x, t) dx$. Using the physical dimension $[x] = L$ and $[c(x, t)] = L^{-(1+d_f)}$ in the expression for dM_{d_f} , we immediately find that it bears no dimension and so does the quantity M_{d_f} . It implies that the numerical value of M_{d_f} remains the same despite the fact that the system evolves with time. On the other hand, the concentration $c(x, t)$ is defined as the number of particles per unit volume of embedding space ($V \sim L^d$ where $d = 1$) per unit mass (M) and hence $[c] = L^{-1}M^{-1}$ [25]. Now applying the principle of equivalence we obtain

$$M(L) \sim L^{d_f}, \quad (38)$$

which is often considered as one of the most commonly used benchmark for defining fractal. An object whose mass-length relation satisfies Eq. (38) with typically a non-integer exponent is said to be a fractal.

In summary, besides solving the model analytically,

we also performed extensive numerical simulation which fully support all theoretical findings. Especially, the conditions under which scaling and fractals emerge are found, the fractal dimensions of the three models are given and the relationship between fractal dimension and conserved quantity is pointed out. Our findings complement the results found in the condensation-driven aggregation indicating that these results are ubiquitous in the aggregation processes where mass conservation is violated. Besides, we show that the interval size distribution function in both variants of DCS exhibits dynamic scaling and we verify it numerically using the idea of data-collapse. We hope this work will provide useful insights and theoretical predictions for various physical, chemical and biological systems that emerge as fractal. It would be instructive to analyze our model with other fragmentation rates described by sum kernel $K(x, y) = x + y$ and product kernel $K(x, y) = xy$. We propose to address these issues in subsequent work.

NIP would like to thank Dhaka University for awarding Bangabondhu Fellowship.

-
- [1] B. B. Mandelbrot, *Fractals: Form, Chance, and Dimension*, Freeman, San Francisco, 1977.
 - [2] B. B. Mandelbrot, *The Fractal Geometry of Nature*, Freeman, San Francisco, 1982.
 - [3] Edgar E. Peters, *Fractal Market Analysis: Applying Chaos Theory to Investment and Economics*, Wiley, New York, 1994.
 - [4] G. Korvin, *Fractal models in the earth sciences*, Amsterdam, Elsevier, 1992.
 - [5] T. Vicsek, *Fractal Growth Phenomena*, Second ed., World Scientific, Singapore, 1992.
 - [6] J. Feder, *Fractals*, Plenum Press, New York, 1988.
 - [7] M. E. J. Newman, Power laws, Pareto distributions and Zipf's law, *Contemporary Physics* 46 (2005) 323.
 - [8] S. Sears, M. Soljagic, M. Segev, D. Krylov, and D. Bergman, Cantor set fractals from solitons, *Phys. Rev. Lett.* 84 (2000) 1902.
 - [9] N. Hatano, Strong Resonance of Light in a Cantor Set, *J. Phys. Soc. Jpn.* 74 (2005) 3093.
 - [10] P. L. Krapivsky and S. Redner, Random walk with shrinking steps, *Am. J. Phys.* 72 (2004) 591.
 - [11] K. Esaki, M. Sato, M. Kohmoto, Wave propagation through Cantor-set media: Chaos, scaling, and fractal structures, *Phys. Rev. E* 79 (2009) 056226.
 - [12] E. Ben-Naim and P. L. Krapivsky, Fragmentation with a Steady Source, *J. Phys. Lett. A* 293 (2000) 48.
 - [13] R. M. Ziff and E. D. McGrady, Kinetics of Polymer Degradation, *Macromolecules* 19 (1986) 2513.
 - [14] P. L. Krapivsky and E. Ben-Naim, Multiscaling in Stochastic Fractals, *Phys. Lett. A* 196 (1994) 168.
 - [15] M. K. Hassan and M. Z. Hassan, Emergence of fractal behavior in condensation-driven aggregation, *Phys. Rev. E*, 79 (2009) 021406.
 - [16] M. K. Hassan, M. Z. Hassan and N. Islam, Emergence of fractal in aggregation with stochastic self-replication, *Phys. Rev. E* 88 (2013) 042137.
 - [17] M. K. Hassan and G. J. Rodgers, Models of fragmentation and stochastic fractals, *Phys. Lett. A* 208 (1995) 95.
 - [18] M. K. Hassan and G. J. Rodgers, Multifractality and multiscaling in two dimensional fragmentation, *Phys. Lett. A* 218 (1996) 207.
 - [19] M. K. Hassan, Multifractality and the shattering transition in fragmentation processes, *Phys. Rev. E*, 54 (1996) 1126.
 - [20] M. K. Hassan, Fractal dimension and degree of order in sequential deposition of mixture, *Phys. Rev. E*, 55 (1997) 5302.
 - [21] P. L. Krapivsky, Kinetics of random sequential parking on a line, *J. Stat. Phys.* 69 (1992) 125.
 - [22] G. I. Barenblatt, *Scaling, Self-similarity, and Intermediate Asymptotics*, Cambridge University Press, 1996.
 - [23] Y. L. Luke, *The special functions and their approximations I*, Academic Press, New York, 1969.
 - [24] F. Family and T. Vicsek, Scaling of the active zone in the Eden process on percolation networks and the ballistic deposition model, *J. Phys. A: Math. Gen.* 18 (1985) L75.
 - [25] C. Connaughton, R. Rajesh, and O. Zaboronski, *Phys. Rev. E* 69 061114 (2004).